Sensors and Actuators A 156 (2009) 95–102

Contents lists available at ScienceDirect

Sensors and Actuators A: Physical

journal homepage: www.elsevier.com/locate/sna

Realization of a wearable miniaturized thermoelectric generator for human body applications

Ziyang Wang[a,b,*], Vladimir Leonov[a], Paolo Fiorini[a], Chris Van Hoof[a,b]

[a] IMEC, Kapeldreef 75, Heverlee 3001, Belgium
[b] ESAT, Kasteelpark Arenberg 10, Heverlee 3001, Belgium

ARTICLE INFO

Article history:
Received 30 September 2008
Received in revised form 17 February 2009
Accepted 17 February 2009
Available online 4 March 2009

Keywords:
Thermoelectric generator (TEG)
Thermopile
Poly-SiGe
Micromachining
Body area networks

ABSTRACT

This paper presents the realization of a full-fledged wearable miniaturized thermoelectric generator (TEG) specifically engineered for human body applications. It is based on a surface micromachined poly-SiGe thermopile. In view of the adverse thermal environment on human body, special attention is paid to the optimal design for the individual thermocouple, for the thermopile featured with a rim structure standing out of Si substrate, and for the wearable TEG. Fabricated by using surface micromachining technology, each thermopile chip contains 2350 or 4700 thermocouples connected thermally in parallel and electrically in series. The effectiveness of the targeted design is validated by both simulation and experiments. To facilitate further packaging, the thermopile chip is flip-chip bonded to a Si chip coated with a thin layer of BCB. Such a bonded thermopile chip delivers an open-circuit output voltage of 12.5 V/(K cm^2) and an output power of 0.026 μW/(K^2 cm^2) on a matched external load. Towards the making of a full-fledged wearable TEG, the bonded thermopile chip is manually assembled with other specially designed components. Being worn on human body, the wearable TEG delivers an open-circuit output voltage of about 0.15 V and an output power of about 0.3 nW on a matched external load. Further improvement in the output performance can be achieved by optimizing material properties, applying metal-to-metal bonding and fabricating thermocouple microstructures on high topography.

1. Introduction

Recent technological advances in integrated circuits, physical sensing and wireless communication have paved the way for the deployment of wearable wireless body area networks (Wireless BAN or WBAN), an enabling technology for continuous health monitoring [1]. A typical wireless body area network is composed of a number of miniature, lightweight, low-power sensing devices, management electronics and wireless transceivers. As an indispensible part of the system, the power supply for these components should be small-sized, lightweight, environment-friendly and everlasting as well. In this context, the traditional batteries and the recent miniaturized fuel cells, both non-rechargeable and rechargeable, are less advantageous than the energy harvesters, especially in terms of effective lifetime and autonomy.

Energy harvesters, also known as energy scavengers, usually capture and convert ambient energy from different forms, such as thermal energy, kinetic energy and electromagnetic energy, into electrical energy [2]. Taking advantage of the Seebeck effect, the thermoelectric generator (TEG) as a type of energy harvester can deliver an electrical output power by converting a heat stream flowing therethrough. Amid the evolution of micromachining technology, a variety of miniaturized TEGs have been made from bismuth telluride (BiTe) compounds, polycrystalline silicon germanium (poly-SiGe) or metals [3–8]. Although ideally BiTe superlattice structures offer a large space for further improvement of the overall thermoelectric properties, characterized by the figure-of-merit *ZT*, the material properties of BiTe compounds practically used in recent miniaturized devices are merely on par with those of poly-SiGe [3–6,9]. Due to the lack of established thin film micromachining technology for BiTe compounds, most of the BiTe-based TEGs are characterized by large dimensions of the individual thermocouple, a relatively small total number of integrated thermocouples and eventually a minimal output voltage [3–6]. Meanwhile, poly-SiGe has been investigated for thermoelectric applications as well due to the wide availability of its thin film processing technology [7,10]. In contrast with BiTe-based TEGs, poly-SiGe based ones normally contain a larger number of individual thermocouples, leading to a higher output voltage under the same temperature difference [7]. However, the much smaller contact area of the poly-SiGe thermocouples gives rise to a more pronounced issue of contact resistance with metal interconnect and consequently a much larger internal electrical resistance.

* Corresponding author at: IMEC, Kapeldreef 75, Heverlee 3001, Belgium. Tel.: +32 16 28 82 22; fax: +32 16 28 10 97.
E-mail address: Ziyang.Wang@imec.be (Z. Wang).

0924-4247/$ – see front matter © 2009 Elsevier B.V. All rights reserved.
doi:10.1016/j.sna.2009.02.028

Moreover, due to the employment of thin film fabrication technology, the height of poly-SiGe thermocouple legs is usually limited, resulting in a minimal thermal resistance.

An adequately large thermal resistance of each thermocouple is crucial to the proper operation of TEG on human body, because of the limited overall temperature difference from human body to the ambient on one hand and the large thermal resistances of human body and the ambient on the other hand. As opposed to the laboratory experimental environment, where a temperature difference can be artificially enforced on the TEG, a TEG being deployed on human body can utilize only a small fraction of an overall temperature difference of 10–15 K. Hence, the output performance of the traditional TEGs, when deployed on human body, is estimated to be inadequate to fulfill the requirements brought by the wireless body area network.

In an attempt to improve TEG output performance, a poly-SiGe based micromachined thermopile has been designed specifically for human body application [11]. Aimed at increasing the thermal resistance of the TEG with regard to human body and the ambient, several measures are taken in the device design for both the individual thermocouple and the whole thermopile. The effectiveness of these measures is validated with modeling and then proved with experimental results obtained on fabricated devices. The output performance of the TEG can be further pushed up by packaging and assembly. In this work, the thermopile chip is first flip-chip bonded to another Si chip of similar size. Thermal measurement under a fixed temperature difference is carried out on the bonded chip with a specially designed experimental set-up. Then the bonded chip is mounted in between a metal plate and a custom designed pin-featured metal radiator. Other accessories, such as wire connection, a wristwatch strap and a shock protection grid, are also mounted. The resulted full-fledged TEG delivers an open-circuit output voltage of about 150 mV on human body at regular office conditions. The output power of this TEG can be improved considerably by further optimizing the material properties of poly-SiGe. The whole development work, including design, modeling, fabrication, measurement and packaging, is described, the final conclusion is drawn and the future work is suggested.

2. Design

2.1. Equivalent circuit model of a TEG deployed on human body

A typical TEG is made up of a number of thermocouples, which are connected electrically in series and thermally in parallel, sandwiched between a bottom chip and a top chip, as schematically shown in Fig. 1.

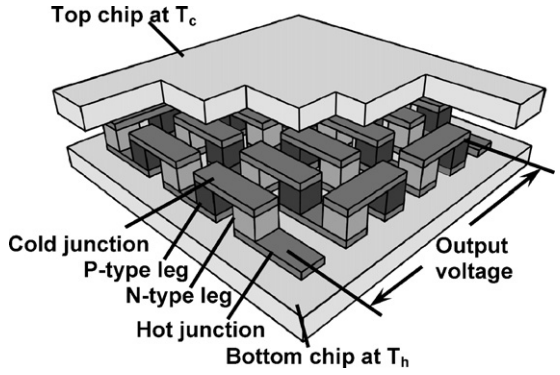

Fig. 1. Schematic configuration of a typical TEG which is made up of a number of thermocouples connected electrically in series and thermally in parallel. The thermocouples are sandwiched between a bottom chip and a top chip.

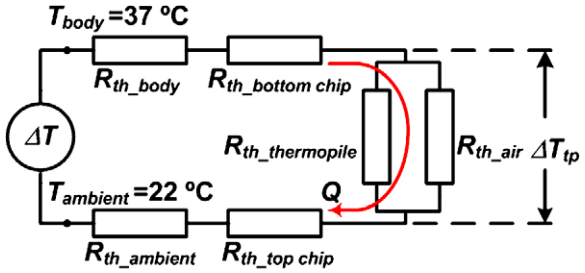

Fig. 2. Equivalent circuit model of a typical TEG deployed on human body.

When there is a temperature difference ΔT_{tp} between the thermocouple junctions, an output voltage V is delivered between the two terminals due to the Seebeck effect:

$$V = n \cdot (\alpha_p - \alpha_n) \cdot \Delta T_{tp} \tag{1}$$

where n is the total number of thermocouples, α_p and α_n are the Seebeck coefficients for p-type and n-type material, respectively. The output power P is dependent on both the TEG electrical resistance R_{TEG} and the electrical resistance of the external load R_L:

$$P = \frac{V^2}{(R_{TEG} + R_L)^2} \cdot R_L = \frac{n^2 \cdot (\alpha_p - \alpha_n)^2 \cdot \Delta T_{tp}^2}{(R_{TEG} + R_L)^2} \cdot R_L. \tag{2}$$

On a matched external load, the optimal power output P_o is obtained as

$$P_o = \frac{V^2}{4R_{TEG}} = \frac{n^2 \cdot (\alpha_p - \alpha_n)^2 \cdot \Delta T_{tp}^2}{4R_{TEG}}. \tag{3}$$

Such a TEG being worn on human body can be analyzed by using the equivalent circuit model illustrated in Fig. 2.

As depicted in Fig. 2, the TEG is connected thermally in series with human body and the ambient. Because of the low thermal conductivity of human skin (namely dermal layer, fatty layer and visceral layer), it constitutes a large thermal resistor in this equivalent circuit [12]. The thermal resistance of the ambient is also large owing to the normally inefficient heat dissipation on the small chip area under a limited temperature difference. In contrast, the thermal resistance of a micromachined TEG is minimal for two reasons. Firstly, each individual thermocouple has a thermal resistance not large enough for applications on human body. This is due to the short thermocouple height, limited by the inability of contact photolithography to resolve fine patterns on a high topography. Secondly, the fact that all the thermocouples are arranged thermally in parallel makes the total thermal resistance even smaller. Consequently, a large portion of the overall temperature difference drops on both human body and the ambient while only a small fraction drops between the junctions of the thermocouples.

As a result of this hostile thermal environment, the design of the TEG in this work is specifically aimed at increasing its thermal resistance. The reduction of the thermal resistances of other components is achieved mainly through proper packaging and smart assembly for the TEG.

2.2. Design of an individual micromachined thermocouple

An individual thermocouple is designed in such a way that its thermal resistance is maximized. As schematically shown in Fig. 3, each thermocouple is composed of p-type and n-type thermocouple legs interconnected by aluminum pads at two junctions (denoted as “A” and “B” in Fig. 3). In this design, several measures have been adopted to maximize the thermal resistance of the thermocouple microstructure. Firstly, a 2.5-μm-deep trench

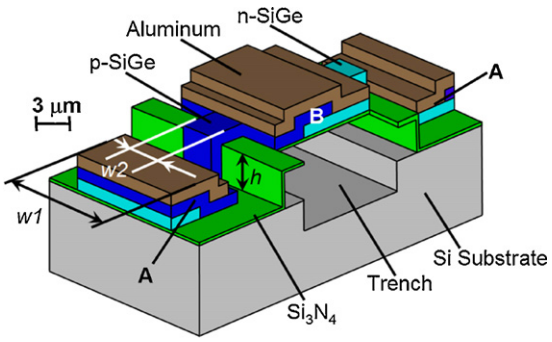

Fig. 3. Schematic design of an individual micromachined poly-SiGe thermocouple.

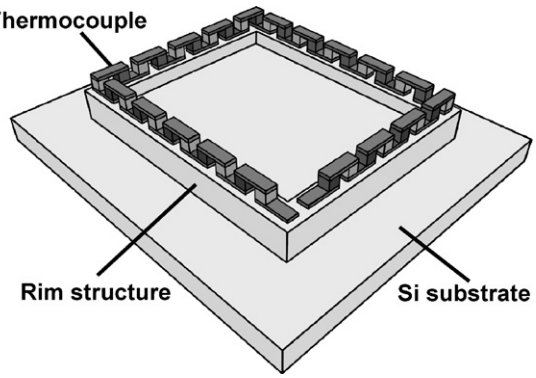

Fig. 4. Schematic illustration of a number of micromachined thermocouples fabricated on top of a 250-μm-high rim structure.

is formed below the junction "B" so as to improve the thermal isolation between two junctions. Secondly, on top of this shallow trench, an extra 0.5-μm-high step is made. Thirdly, the width of thermocouple leg (denoted as *w*2 in Fig. 3) is narrowed down to the technological limit while the width of the junction area (denoted as *w*1 in Fig. 3) is kept relatively large so as to reduce the contact resistance. The typical dimensions for *w*1 and *w*2 are 10 μm and 3 μm, respectively. The footprint area of such a thermocouple is 30 μm × 16 μm.

2.3. Design of the micromachined thermopile

The arrangement of the thermopile is differentiated from previous ones [3–8] by mounting the micromachined thermocouples on top of a 250-μm-high rim structure made by deep reactive ion etching (DRIE) into the Si substrate (Fig. 4). With all the other parameters kept the same, the formation of this rim structure significantly increases the average air gap thickness, compared to the traditional configuration. Thus, the thermal resistance of the air gap between the two chips, which is thermally in parallel with the thermopile, is also increased significantly. In an optimized configuration, the thermal resistance of the ensemble of the thermocouples must match that of the air gap between the two chips [13]. Such a condition is attained by appropriately varying the total number of thermocouples. In our design, thermal resistances are matched with a configuration consisting of about 2000 thermocouples.

As illustrated in Fig. 2, larger thermal resistances of the air gap and of the thermopile result in a larger temperature difference across the thermopile and hence a better output performance as well.

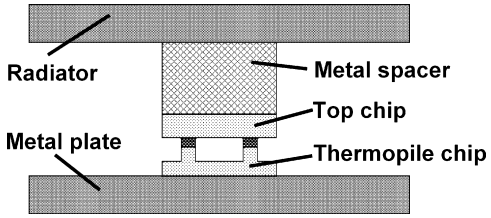

Fig. 5. Schematic arrangement of the TEG, which essentially consists of a metal plate, a flip-chip bonded thermopile chip, a metal spacer and a radiator from bottom to top.

2.4. Design of the TEG

The proper design of the TEG is carried out with a twofold purpose. On one hand, the package of the TEG is needed to reduce the thermal resistances of human body and the ambient. On the other hand, it should also facilitate easy and convenient deployment on human body. The first purpose is fulfilled by first connecting the thermopile chip to a Si chip of similar size and then inserting the bonded chip in between a larger metal plate and a pin-featured radiator. The conceptual design is schematically depicted in Fig. 5. The second purpose is achieved by custom shaping the metal plate and connecting a conventional wristwatch strap to it.

3. Modeling

The modeling of the designed TEG is implemented in a hybrid manner. Finite element modeling (FEM) is used to analyze the characteristics of an individual micromachined thermocouple while analytical modeling with the equivalent circuit is employed to pro-

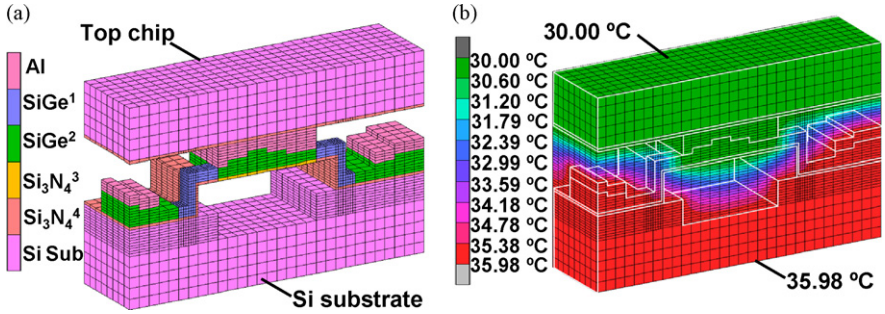

Fig. 6. (a) Cross-sectional view of the 3D FEM model for an individual thermocouple bonded to a top chip (the air gap is removed for clarity); for ease of building the FEM model, SiGe is distinguished based on the width: [1] 3-μm-wide SiGe structure and [2] 10-μm-wide SiGe structure; so is the case for Si_3N_4: [3] 10-μm-wide Si_3N_4 and [4] 16-μm-wide Si_3N_4; (b) Cross-sectional view of the temperature distribution in the thermocouple with a fixed temperature (30 °C) at the top surface and a fixed heat flux (100 mW/mm^2) injected into the bottom surface.

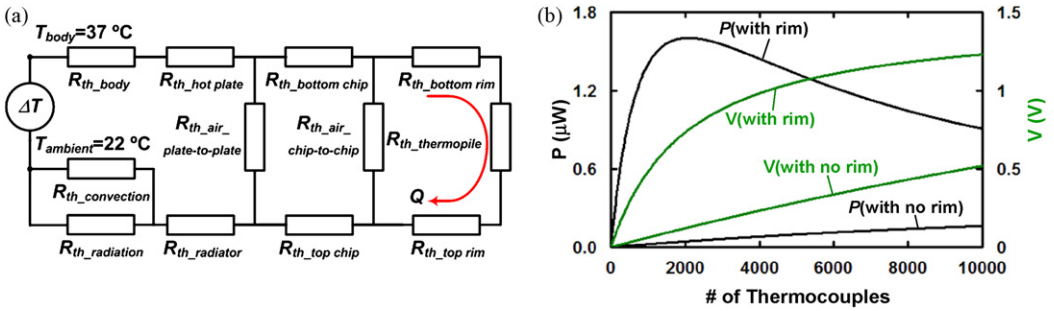

Fig. 7. (a) Equivalent circuit model of a full-fledged TEG deployed on human body; (b) Ideal output performance of the designed TEG with and with no rim structure formed.

vide an estimate of the output performance from the TEG. In the analytical modeling, the results obtained from the FEM are used as a known input. This hybrid modeling combines the accuracy of FEM in analyzing the complex microstructure of thermocouple with the efficiency of analytical modeling thanks to reasonable simplification.

3.1. Finite element modeling

A fully 3D model of an individual thermocouple bonded to a top chip is built with FEM software MSC.Marc according to the actual dimensions, as shown in Fig. 6(a). With the 3D FEM model, the thermal resistance of this structure, which cannot be determined easily with analytical model, can be calculated by fixing the temperature at the top surface and injecting a known heat flux into the bottom surface. The temperature distribution in the thermocouple with these boundary conditions is illustrated in Fig. 6(b). It can be observed that the temperature distribution in the Si part is homogeneous due to its large thermal conductivity. The temperature difference, as indicated by the spectrum of colors, is mainly concentrated across the air gap and the narrow vertical thermocouple legs. From the overall temperature difference between two surfaces and the total heat flow, the thermal resistance can be calculated. For instance, an individual thermocouple with 3-μm-high thermocouple legs has a thermal resistance of 1.25×10^5 K/W after the sacrificial layer is completely removed.

3.2. Analytical modeling

In the analytical modeling for the whole device, the thermocouples are simplified to be a homogeneous layer with extracted properties from the FEM results. Hence, the designed TEG, as depicted in Fig. 5, deployed on human body can be modeled by using equivalent circuit model shown in Fig. 7(a). The equivalent circuit is composed of a number of thermal resistors representing various components in the TEG. Across the various thermal resistors, a voltage source symbolizing the overall temperature difference between human body and the ambient is enforced. The temperatures for human body and the ambient are assumed to be 37 °C and 22 °C, respectively. As shown in Fig. 7(b), the output voltage and power transferred into matched external load from the TEG are plotted against the total number of thermocouples. The output performances with and with no rim structure are compared in the same figure. By making the rim structure, the output voltage is increased by a variable factor no less than 2, depending on the total number of thermocouples. The maximum output power is reached in a TEG containing around 2000 thermocouples. With the ideal poly-SiGe material properties (e.g., a *ZT* larger than 0.1 for both p-type and n-type poly-SiGe) and for the optimal TEG configuration (e.g., 3-μm-high thermocouple leg, metal-to-metal bonding from thermopile chip to top chip, minimal parasitic thermal resistance between components), the maximum power output can exceed 1.5 μW on a matched external load.

4. Fabrication

The poly-SiGe based thermopile is fabricated by using surface micromachining technology, as illustrated in Fig. 8. Firstly, a shallow trench as deep as 2.5 μm is etched into an 8-inch Si substrate (Fig. 8(a)). Then a double tetraethyl orthosilicate (TEOS) deposition is implemented: the first one is used to fill the shallow trench while the second one is used to form a 0.5-μm-high vertical step (Fig. 8(b)). The TEOS layer serves as a sacrificial material, which is removed afterwards by BHF. On top of the TEOS layer, a thin Si_3N_4 layer is deposited for encapsulation (Fig. 8(c)). Following the Si_3N_4

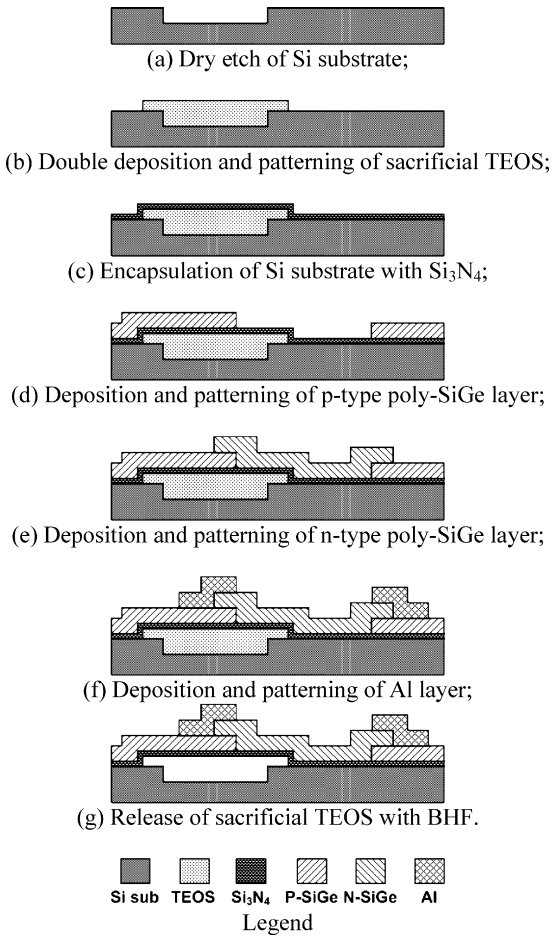

Fig. 8. Schematic fabrication process for the micromachined thermopile.

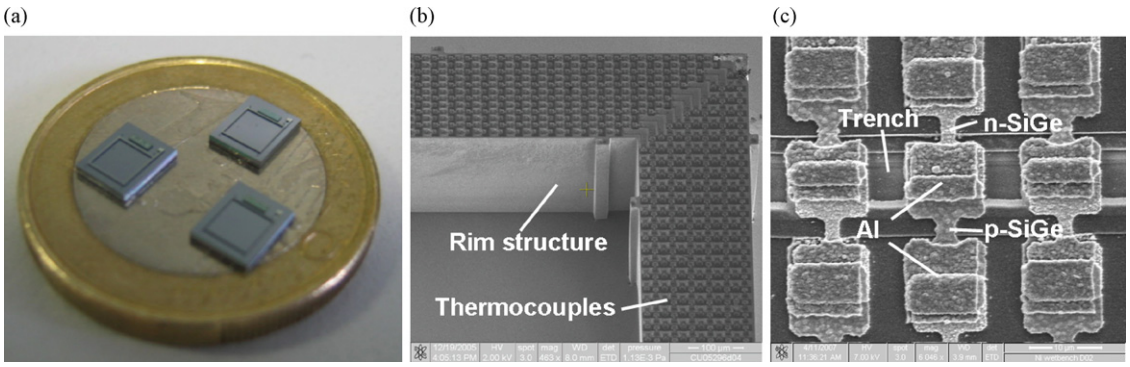

Fig. 9. (a) Photo of micromachined thermopile chips placed on one Euro coin; (b) SEM micrograph of the rim structure, on top of which thousands of thermocouples are fabricated in a daisy chain; (c) Close-up view of the micromachined thermocouples.

deposition, in-situ doped p-type and n-type poly-SiGe layers are deposited by low temperature chemical vapor deposition (LPCVD) and then patterned by photolithography and dry etch, respectively, to shape the thermocouple legs (Fig. 8(d) and (e)). Next, the poly-SiGe layer surface is thoroughly cleaned with BHF and argon plasma, immediately succeeded by aluminum sputtering and patterning to interconnect thermocouple legs electrically (Fig. 8(f)). In order to facilitate the release of sacrificial layer, the thin Si_3N_4 layer in between adjacent thermocouples is opened with dry etch. Sequentially, Si substrate is etched deeply to form the rim structure. Finally, the thermopile chip is released in BHF solution and dried with critical point dryer to avoid stiction (Fig. 8(g)).

The fabricated thermopile chips are shown in Fig. 9(a). Each chip measures 4 mm × 4 mm. The 250-μm-high rim structure standing out of the Si substrate can be clearly observed. Each chip contains either 2350 or 4700 thermocouples connected electrically in series. SEM micrographs showing an overview of the rim structure and a close-up view of the individual thermocouples are given in Fig. 9(b) and (c).

The relevant material properties of poly-SiGe have been characterized [14]. As shown in Table 1 the figure-of-merit *ZT* for p-type and n-type poly-SiGe is respectively 0.01 and 0.05. The specific contact resistance between n-type poly-SiGe and metals is larger than the desired value of 200 Ω μm^2 by a factor of more than 100. Due to the minimal contact area between poly-SiGe and metals, the electrical resistance of each individual thermocouple designed with the typical dimensions (10 μm for *w*1 and 3 μm for *w*2) can be as large as 2.5 kΩ. A thermopile containing several thousand of such thermocouples can exhibit a total electrical resistance of larger than 10 MΩ.

Table 1
Summary of material properties for LPCVD poly-SiGe.

	p-type	n-type
Seebeck coefficient (μV/K)	35	−190
Electrical resistivity (mΩ cm)	1.1	6.2
Thermal conductivity (W/m/K)	3.5	3.5
Figure-of-merit *ZT*	0.01	0.05
Specific contact resistance with AlCu (Ωμ m^2)	78	5.5×10^4
Specific contact resistance with Ti/Cu (Ωμ m^2)	57	2.9×10^4

5. Measurement

Measurement of output voltage from the micromachined thermopile has been implemented at various stages of the development

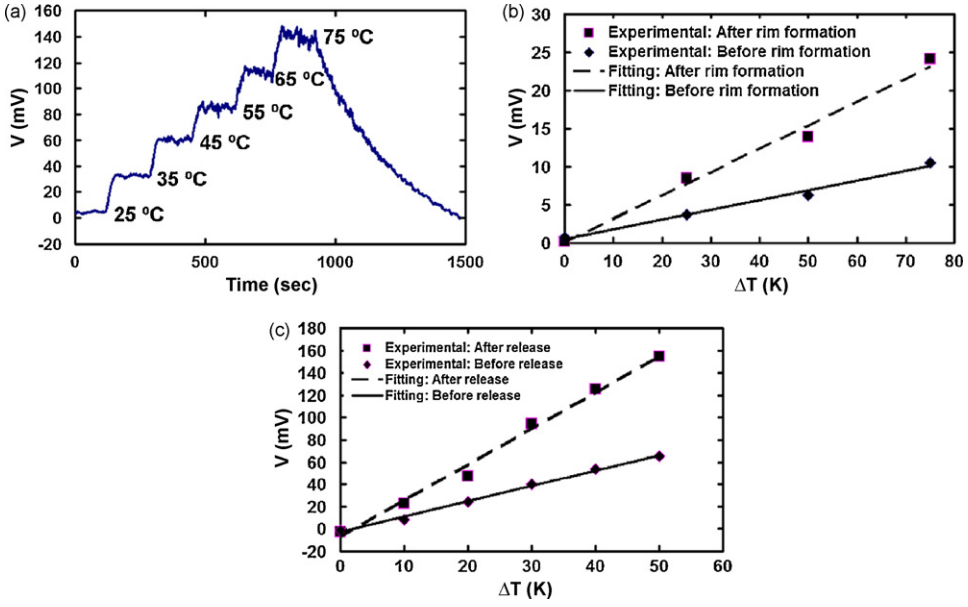

Fig. 10. (a) Open-circuit output voltage of a micromachined thermopile at various temperatures of the thermal chuck; (b) Open-circuit output voltages plotted against the overall temperature difference from the thermal chuck to the ambient before and after rim formation; (c) Open-circuit output voltages plotted against the overall temperature difference from the thermal chuck to the ambient before and after BHF sacrificial release.

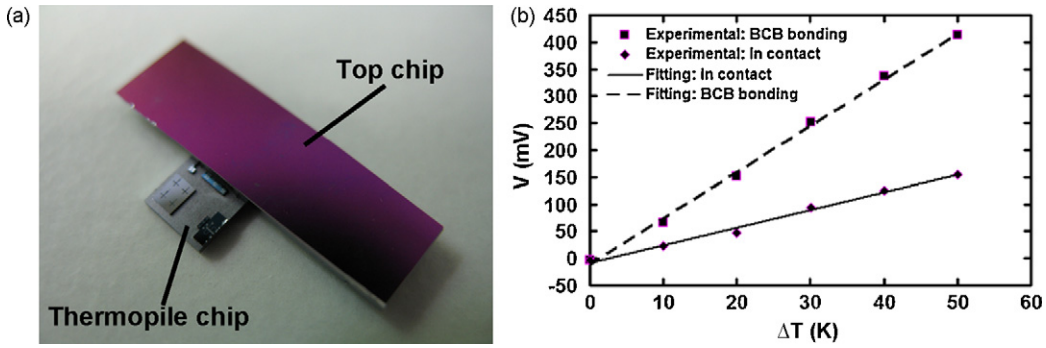

Fig. 11. (a) Photo of the thermopile chip bonded to a top Si chip; (b) Open-circuit output voltages plotted against the overall temperature difference from the thermal chuck to the ambient with loose thermal contact and BCB flip-chip bonding.

work. As a quick characterization method, the measurement is performed on a standard parametric analyzer equipped with a thermal chuck. The thermopile chip is first fixed onto the chuck by vacuum and then heated up by the underlying chuck. Another Si chip as a radiator is gently placed on top of the thermopile chip. The output voltage delivered between two terminals of the daisy chain of thermocouples is measured as the temperature of the thermal chuck increases. As shown in Fig. 10(a), the output voltage proportionally increases with the temperature. Fig. 10(b) illustrates the effectiveness of rim formation in improving the output performance. By making the rim structure, the output voltage under the same overall temperature difference between the thermal chuck and the ambient is increased by a factor no less than 2. The magnitude of this improvement is consistent with modeling result. Fig. 10(c) demonstrates the effectiveness of BHF sacrificial release, which further boosts the output voltage by a factor of about 2.5. These results experimentally prove the validity of the proposed design.

6. Packaging and assembly

The released thermopile chip is bonded to a BCB-coated Si chip on the Karl Süss flip chip bonder FC6. Compared to metal-to-metal bonding, BCB bonding is implemented at a smaller pressure and a lower temperature, effectively reducing the probability of damaging the thermocouple microstructure. However, BCB has a much lower thermal conductivity than metals. For instance, the thermal conductivity of Cyclotene 4000 series BCB resin, which is used in this work, is 0.29 W/(m K). To mitigate the thermal isolation introduced by the BCB layer, its thickness needs to be minimized. Thus in this work, a low-viscosity resin type is used and the thickness of the coated BCB layer on the top chip is reduced to about 1 μm. The thermopile chip after flip-chip bonding is shown in Fig. 11(a). In comparison with the case where the top Si chip is only placed on the thermopile chip, the output performance after flip-chip bonding further increases by a factor of about 2.5, as indicated in Fig. 11(b).

To allow a performance comparison with other reported thermopiles, a measurement set-up has been manufactured so as to enforce and meanwhile measure the temperature difference between the bottom and the top surface of the bonded thermopile chip. As shown in Fig. 12(a), the gap in between the two large aluminum blocks can be tuned by moving the top block along the four plastic tracks. The bonded thermopile chip is placed in between the two blocks by using thermal epoxy. By gently moving the top block down towards the bottom one along the tracks, a close but not damaging contact with the bonded chip is ensured. In the thermal experiment, the bottom block is heated up while the top block is kept at almost the same temperature due to its large thermal capacity. Thus, a temperature difference is created artificially between the bottom and the top surface of the bonded thermopile chip. Moreover, this temperature difference is gauged by employing a commercial thermocouple. The measured output voltage of the bonded thermopile chip is plotted in Fig. 12(b) against the temperature difference. Under a unit temperature difference of 1 K, the open-circuit output voltage is about 0.25 V. This indicates that the open-circuit output voltage per unit temperature difference per unit area is 12.5 V/(K cm^2). The output power delivered on a matched external load amounts to 0.026 μW/(K^2 cm^2).

The final assembly of the TEG is accomplished manually. The thermopile chip is attached to a specially shaped metal plate by using thermally epoxy, as displayed in Fig. 13(a). Then wires are bonded to connect the metal pads on the chip to an adjacent printed circuit board (PCB). After that, a metal spacer is fixed on top of the

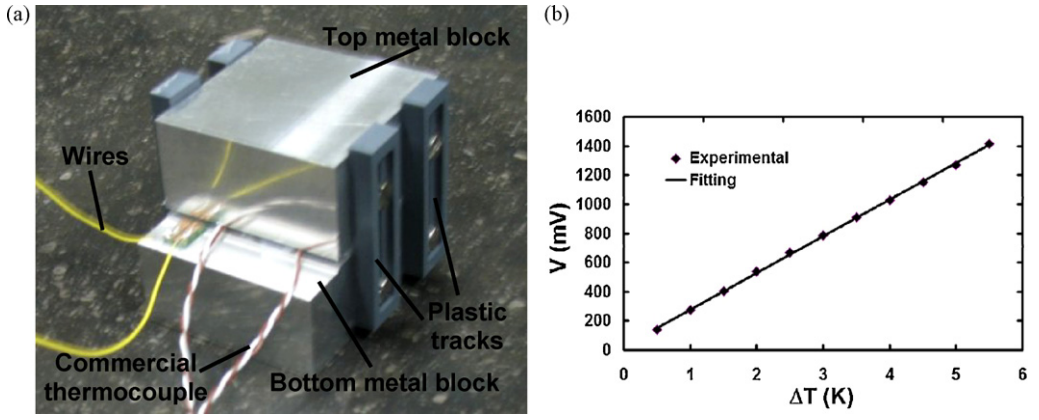

Fig. 12. (a) Photo of the experimental set-up for thermal measurement under a fixed temperature difference; (b) Open-circuit output voltage plotted against the temperature difference between the bottom and the top surface of the bonded thermopile chip.

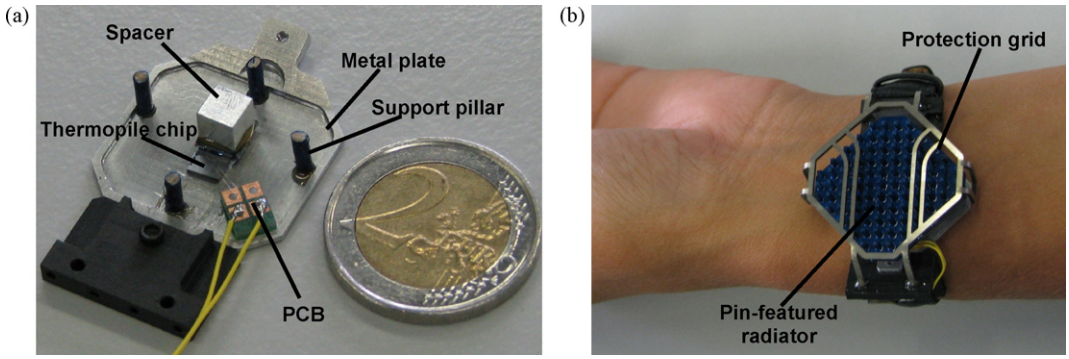

Fig. 13. Photos of the wearable TEG for human body applications: (a) TEG being assembled; (b) TEG being worn on human body.

thermopile chip to increase the gap in between the metal plate and the top radiator. Four thermally isolating pillars are placed around the thermopile chip for mechanical support. Next, a top radiator featured with an array of pins is fixed onto the metal spacer and the pillars, as shown in Fig. 13(b). Finally, a wristwatch strap is joined to the metal plate and a shock protection grid is mounted. This TEG delivers an open-circuit output voltage of about 150 mV when being worn on wrist at regular office conditions. The actual temperature difference dropping between the junctions of the poly-SiGe thermocouple is estimated to be 0.15 K. Because the internal electrical resistance is too high, i.e. about 20 MΩ, the output power delivered on a matched external load is estimated to be about 0.3 nW. This result indicates that the output power is basically limited by the large specific contact resistance formed between n-type poly-SiGe and metal layers.

7. Conclusion and outlook

This paper describes the various steps in the development of a full-fledged TEG for human body applications. In view of the thermal environment on human body, special attention is paid to the optimal design for the individual thermocouple, for the thermopile containing a large number of thermocouples and for the wearable TEG device. A hybrid model combining the FEM and the analytical equivalent circuit is built to evaluate device performance and optimize design. The thermopile is fabricated by using surface micromachining technology. Results from thermal and electrical measurements at various stages of fabrication have demonstrated the effectiveness of the design strategies adopted to improve thermal isolation. After complete fabrication, the thermopile chip is permanently attached to another Si chip by flip-chip bonding. Thermal measurement, implemented with a specially designed experimental set-up, on the bonded thermopile chip reveals that the open-circuit output voltage is 12.5 V/(K cm^2). Moreover, the output power delivered on a matched external load amounts to 0.026 μW/(K^2 cm^2). Then manual assembly work on the bonded chip and other custom designed components, such as the metal plate, the pin-featured radiator and the protection grid, is performed to realize a full-fledged TEG. Being worn on wrist, the TEG delivers a stable output voltage of around 150 mV at regular office conditions. Connected to a matched external load, it is estimated to produce an output power of about 0.3 nW.

Future work will be focused on further improving the output performance of TEG. Firstly, the internal electrical resistance needs to be minimized by reducing the specific contact resistance between n-type poly-SiGe and metal layers. Given a much lower contact resistance, the output power from the same TEG can be significantly increased. Secondly, the BCB bonding needs to be replaced by metal-to-metal bonding, because a metal layer has a much higher thermal conductivity than a BCB layer. Thirdly, the current planar thermocouple microstructure needs to be upgraded into a high-topography one, which is thermally more efficient for human body applications [15].

Acknowledgements

The authors would like to thank IMEC colleagues, in particular A. Verbist, B. Du Bois, T. Borgers for technical assistance in processing; Dr. N. Posthuma for help in material development; H. Oprins for assistance in finite element simulation; and M. Van Dievel for technical assistance in electrical measurement.

References

[1] E. Jovanov, A. Milenkovic, C. Otto, P.C. de Groen, A wireless body area network of intelligent motion sensors for computer assisted physical rehabilitation, J. NeuroEng. Rehab. (2005) 26.
[2] N.S. Hudak, G.G. Amatucci, Small-scale energy harvesting through thermoelectric, vibration, and radiofrequency power conversion, J. Appl. Phys. 103 (2008) 101301–102122.
[3] M. Kishi, H. Nemoto, T. Hamao, M. Yamamoto, S. Sudou, M. Mandai, S. Yamamoto, Micro-thermoelectric modules and their application to wristwatches as an energy source, in: Proceedings of 18th International Conference on Thermoelectrics, Baltimore, USA, August 29 to September 2, 1999, pp. 689–692.
[4] G.J. Snyder, J.R. Lim, C.-K. Huang, J.-P. Fleurial, Thermoelectric microdevice fabricated by a MEMS-like electrochemical process, Nat. Lett. 2 (2003) 528–531.
[5] H. Böttner, J. Nurnus, A. Gavrikov, G. Kühner, M. Jägle, C. Künzel, D. Eberhard, G. Plescher, A. Schubert, K.-H. Schlereth, New thermoelectric components using microsystem technologies, IEEE J. MEMS 13 (2) (2004) 414–420.
[6] L.M. Goncalves, C. Couto, P. Alpuim, J.H. Correia, Thermoelectric micro converters for cooling and energy scavenging systems, J. Micromech. Microeng. 18 (2008) 064008–64015.
[7] M. Strasser, R. Aigner, C. Lauterbach, T.F. Sturm, M. Franosch, G. Wachutka, Micromachined CMOS thermoelectric generators as on-chip power supply, Sens. Actuators A 114 (2004) 362–370.
[8] W. Glatz, S. Muntwyler, C. Hierold, Optimization and fabrication of thick flexible polymer based micro thermoelectric generator, Sens. Actuators A 132 (2006) 337–345.
[9] R. Venkatasubramanian, E. Siivola, T. Colpitts, B. O'Quinn, Thin-film thermoelectric devices with high room temperature figure of merit, Nature 413 (2001) 597–602.
[10] D.D.L. Wijngaards, R.F. Wolffenbuttel, Thermo-electric characterization of APCVD poly$Si_{0.7}Ge_{0.3}$ for IC-compatible fabrication of integrated lateral Peltier elements, IEEE Trans. Elec. Devices 52 (5) (2005) 1014–1025.
[11] Z. Wang, V. Leonov, P. Fiorini, C. Van Hoof, Realization of a poly-SiGe based micromachined thermopile, in: Proceedings of Eurosensors'08, Dresden, Germany, September 7–10, 2008, pp. 1420–1423.
[12] Z. Wu, H.H. Liu, L. Lebanowski, Z. Liu, P.H. Hor, A basic step toward understanding skin surface temperature distributions caused by internal heat sources, Phys. Med. Biol. 52 (2007) 5379–5392.
[13] V. Leonov, P. Fiorini, Thermal matching of a thermoelectric energy scavenger with the ambient, in: Proceedings of 5th European Conference on Thermoelectrics, Odessa, Ukraine, September 10–12, 2007, pp. 129–133.
[14] Z. Wang, P. Fiorini, V. Leonov, C. Van Hoof, Characterization of poly-$Si_{70\%}Ge_{30\%}$ for surface micromachined thermopiles, in: Proceedings of PowerMEMS'08, Sendai, Japan, November 9–12, 2008, pp. 23–26.
[15] J. Su, R.J.M. Vullers, M. Goedbloed, Y. Van Andel, R. Pellens, C. Gui, V. Leonov, Z. Wang, Process development on large-topography microstructures for thermoelectric energy harvesters, in: Proceedings of PowerMEMS'08, Sendai, Japan, November 9–12, 2008, pp. 365–368.

Biographies

Ziyang Wang received his Bachelor of Engineering and Master of Engineering degrees from Department of Precision Instruments in Tsinghua University in Beijing, China, in 2002 and 2004, respectively. His master thesis was about the development of surface micromachined micromirror array. As from September, 2004, he has been affiliated with IMEC and meanwhile Department of Electrical Engineering (ESAT) in Catholic University of Leuven to pursue his PhD degree. His PhD Dissertation is about the development of poly-SiGe based micromachined thermoelectric generator for human body applications. His research interests include miniaturized thermoelectric devices, CMOS-MEMS integration and advanced processing technology in MEMS.

Vladimir Leonov was born in St. Petersburg, Russia, in 1958. He received the Ph.D. Degree in optical devices from the State Optical Institute, St. Petersburg, where he worked as a Senior Scientist during 1981–1998 on thermal detectors and arrays. In 1998–2000 he was with Southern Methodist University, Dallas, TX, where he worked on pyroelectric infrared arrays for Raytheon. In 2000–2003 he was a Principal Scientist at XenICs, Leuven, Belgium, and starting in 2003, he is a Senior Scientist at IMEC. He has authored over 110 publications and 14 patents. His major interests are concentrated on energy scavengers (power MEMS), electrets and poly-SiGe infrared arrays.

Paolo Fiorini was born in Rome, Italy, in 1953. He received his Ph.D. Degree in physics from the University of Rome, Italy, in 1977. He has been active in the field of electrical and optical properties of semiconductors for many years, working at the University of Rome, where he was Associated Professor in Solid State Physics until 2000. Since then he is at IMEC, International Microelectronic centre, Leuven, Belgium, where he is performing research in the field of Microsystems. He devoted particular attention to micromachined IR detectors operating at room temperature and to energy harvesting devices for application in autonomous sensor networks.

Chris Van Hoof is Program Director (Integrated Systems and Smart Implants) and Associate Department Director at IMEC in Leuven, Belgium. His work focuses on the application of advanced packaging and interconnect technology (2D and 3D integration, RF integration) and ultra-low power design technology for the creation of integrated systems, ultra-low power wireless autonomous sensor systems and smart implantable devices. After a Ph.D. in Electrical Engineering (University of Leuven, 1992) in collaboration with IMEC, he became successively Head of the Detector Systems Group (in 1998), Director of the Microsystems and Integrated Systems Department (in 2002), and Program Director (in 2007). He is a laureate of the Belgian Royal Academy of Sciences and since 2000 a part-time professor at the University of Leuven.